Physicochem. Probl. Miner. Process., 62(4), 2026, 231288

http://www.journalssystem.com/ppmp

Physicochemical Problems of Mineral Processing

ISSN 1643-1049

Study on the screening and interaction mechanism of collectors for acanthite based on frontier orbital theory

Li-qiang Lin [1], Ting-sheng Qiu [1,2], Guan-fei Zhao [1,2], Kai-wei Ding [3], Lai-chang Zou [4], Zhong-mei Sun [4]

[1] School of Resources and Environmental Engineering, Jiangxi University of Science and Technology, Ganzhou, 341000, China

[2] Jiangxi Provincial Key Laboratory of Low-Carbon Processing and Utilization of Strategic Metal Mineral Resources, Jiangxi University of Science and Technology, Ganzhou, 341000, China

[3] Central South University, Changsha, 410000, China

[4] Zijin Mining Group Co., Ltd., Longyan, 364200, China

Corresponding author: fly.guan@163.com (GF.Zhao)

Abstract: The collecting performance of four typical sulfide collectors—sodium butyl xanthate (SBX), ammonium dibutyl dithiophosphate (ADD), sodium diethyl dithiocarbamate (DDTC), and O-isopropyl-N-ethyl thionocarbamate (Z-200)—with acanthite (Ag2S) was investigated using DFT calculations, frontier orbital analysis, and flotation tests. Frontier orbital matching and energy difference calculations reveal that ADD forms a σ-bond with the LUMO of three-coordinated Ag and a back-donating π-bond with the HOMO of four-coordinated Ag on acanthite. ADD exhibits the smallest HOMO–LUMO energy gap with acanthite (ΔE_1 = 0.1438 eV) and weaker adsorption energies toward Zn^{2+} and Fe^{2+} than SBX and DDTC. Single-mineral flotation confirmed that ADD achieves the highest acanthite recovery (~85%), while mixed-mineral flotation showed that ADD significantly improves silver grade (19.56% vs. 16.08%) and recovery (85.91% vs. 73.30%) compared to SBX, while effectively depressing sphalerite (Zn recovery 31.79% vs. 69.14%). Combined theoretical and experimental results demonstrate that ADD exhibits both strong collecting ability and high selectivity, making it a promising collector for associated silver sulfide ores. The frontier orbital-based screening approach provides a theoretical foundation for designing specialized collectors for silver minerals.

Keywords: acanthite, dithiophosphate collectors, frontier orbital theory, density functional theory, flotation

1. Introduction

Acanthite (Ag_2S), an important silver sulfide mineral, is one of the primary forms of silver in nature and is commonly found as an associated mineral in various Cu-Pb-Zn polymetallic sulfide deposits (Guner et al., 2024; Neisiani and Chelgani, 2024; Ding et al., 2025). Silver, as a precious metal, exhibits exceptional electrical and thermal conductivity, chemical stability, and unique optical properties (Gong et al., 2024; Wang et al., 2024), rendering it indispensable in electronics, photovoltaics, high-end manufacturing, jewelry, and medical antibacterial applications, and it is often referred to as the "vitamin" of modern industry (Tercero et al., 2019; Chegini et al., 2024; Sverdrup et al., 2014). With the rapid advancement of high-tech sectors, global silver demand has been steadily increasing, intensifying the supply–demand imbalance. Silver minerals exhibit a strong affinity for sulfur and predominantly occur as associated phases in nature (Tiu et al., 2023), among which silver sulfides account for approximately 90% of the total associated silver resources, whereas independent silver deposits are rare. Currently, silver is mainly recovered as a by-product from complex polymetallic sulfide ores, such as lead–zinc deposits (Li et al., 2020; Tkachev et al., 2017). However, the recovery efficiency of associated silver minerals remains generally low, resulting in substantial silver loss in tailings and consequent

DOI: 10.37190/ppmp/231288

resource waste and economic penalties (Zhang and Chen, 2021). Therefore, improving the recovery of associated silver minerals is of both strategic and economic significance.

In sulfide flotation, well-established reagent schemes have been developed for the efficient recovery of base metals such as copper, lead, and zinc (Pienaar et al., 2019). Commonly used collectors include xanthates (e.g., SBX), dithiophosphates (e.g., ADD), esters (e.g., Z-200), and thiocarbamates (e.g., DDTC) (Makanza et al., 2008; Yang et al., 2019; Ignatkina et al., 2010). The selection of these reagents is primarily dictated by the surface physicochemical properties of the target base-metal minerals and their flotation response. For instance, xanthates or ester collectors are commonly employed in copper–sulfur flotation (Vrlíková et al., 2020), whereas dithiophosphates or thiocarbamates with better selectivity are preferred in lead–zinc separation (Ignatkina et al., 2015). Although in the above systems, associated silver sulfide minerals such as acanthite can also enter the concentrate products to some extent along with the main minerals, this recovery approach is relatively inefficient. Due to the lack of specific collectors targeting the surface characteristics of silver minerals, the difference in floatability between silver and other sulfide minerals (e.g., pyrite and sphalerite) is insufficient, resulting in low separation selectivity (Chen and Jun, 2017). Especially in complex polymetallic ore flotation systems, where the surface properties of various minerals are similar, conventional collectors cannot achieve selective enrichment of silver minerals (Acarkan et al., 2011). Regardless of the type of base-metal sulfide deposit, acanthite is invariably recovered together with the primary metals via flotation (Drif et al., 2018; Zhang et al., 2024). Thus, employing first-principles density functional theory (DFT) to elucidate the interaction mechanism between collectors and acanthite at the microscopic level, and thereby to screen or design highly selective collectors, represents a critical pathway toward improving associated silver recovery (Ding et al., 2024).

The selectivity of collector molecules is predominantly governed by their polar groups. Recent studies have demonstrated that metal ions exposed on sulfide mineral surfaces can form strong covalent interactions with the polar groups of collectors (Li et al., 2020; Foucaud et al., 2019; Hung et al., 2004). The formation of such covalent bonds is fundamentally controlled by the effective matching of frontier orbital energies—specifically, when the highest occupied molecular orbital (HOMO) energy of the collector approaches the lowest unoccupied molecular orbital (LUMO) energy of the mineral surface, or vice versa (Cui et al., 2020). A small energy difference facilitates effective orbital overlap and electron transfer across the interface, leading to stable shared-electron-pair bonds and chemisorption (Chen and Li, 2022). With the aid of DFT, the geometric configuration and frontier orbital properties of collector polar groups can be accurately calculated, enabling an in-depth understanding of the adsorption mechanism at the electronic level and a rational assessment of collector performance (Zhang et al., 2022; Zhang et al., 2024b; Feng et al., 2024).

In this study, four representative sulfide collectors, namely SBX, ADD, DDTC, and Z-200, were selected. Their geometries and electronic properties were calculated via DFT using the DMol³ module in Materials Studio, aiming to provide a theoretical basis for screening effective collectors for acanthite.

2. Experimental

2.1. Materials and reagents

All mineral samples used in the experiments were hand-picked and purified. The pure mineral samples of acanthite, sphalerite, and pyrite were obtained from Henan, Hunan, and Yunnan provinces, respectively. The samples were coarsely crushed using a rotary crusher, then dry-ground using a three-head grinder, and subsequently screened through standard sieves. Finally, the size fraction of −0.074 mm +0.038 mm was selected for single-mineral flotation tests. X-ray diffraction (XRD) analysis results (Fig. 1) show that the acanthite sample exhibits characteristic diffraction peaks of acanthite; the sphalerite sample presents only characteristic peaks of sphalerite without obvious impurity phases; and the pyrite sample clearly displays the characteristic diffraction pattern of pyrite. Chemical composition analysis (Table 1) indicates that the purities of acanthite, sphalerite, and pyrite are 90.56%, 96.83%, and 96.84%, respectively, meeting the requirements for single-mineral flotation tests.

2.2. Density Functional Theory calculation method (DFT)

In this study, geometric optimization of four collector molecules (SBX, ADD, Z-200, and DDTC) was performed using the DMol³ module in Materials Studio 2020 software within the framework of density

functional theory. The convergence criteria set for the geometric optimization were as follows: energy change convergence threshold of 2.7×10^{-4} eV/atom (i.e., 1.0×10^{-5} Ha); atomic force convergence threshold of 0.54 eV/atom; atomic displacement convergence threshold of 0.005 Å; SCF iteration number set to 999 with a convergence accuracy of 1.0×10^{-6} eV/atom; density mixing charge parameter set to 0.2, and DIIS size set to 6. The exchange-correlation functional used in the optimization calculations was GGA-PBE, the basis set was DNP 4.4, and the Grimme module was employed for DFT-D correction. The COSMO solvation model was adopted for all collector molecules, using an aqueous environment as the simulation medium (Wang et al., 2024; Shi et al., 2023).

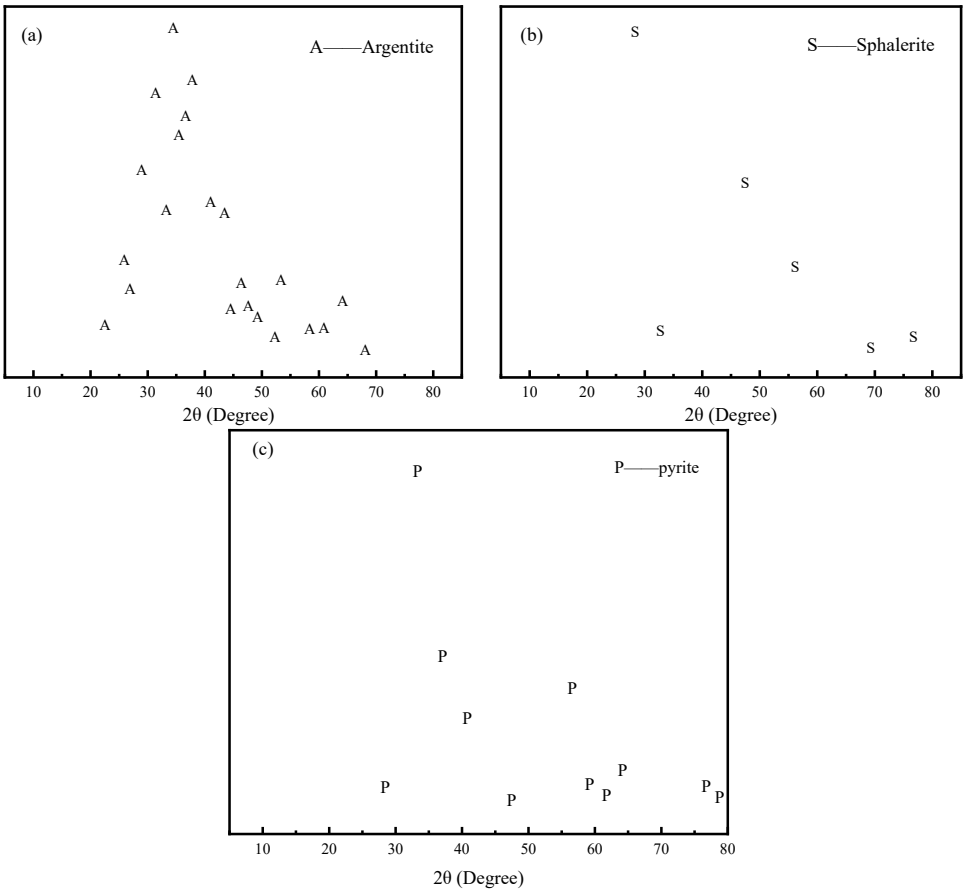

Fig. 1. XRD analysis results of acanthite, sphalerite and pyrite

Table 1. Chemical analysis of pure mineral samples (%)

Sample	Elemental Mass Concentration(%)				Purity
	Ag	Zn	Fe	S	
acanthite	78.88	-	-	12.87	90.56
sphalerite	-	64.97	-	31.91	96.83
pyrite	-	-	46.04	51.64	96.84

2.3. Flotation experiments

Single-mineral flotation tests were conducted using an XFG Ⅱ hanging-cell flotation machine with a 40 mL cell. In each test, 2.0 g of pure mineral sample was weighed, placed in a beaker with an appropriate amount of deionized water, ultrasonically cleaned for 3 min, and then allowed to settle. After removal of the supernatant, the sample was transferred to the flotation cell, and the pulp volume was adjusted to 40 mL. The pH regulator, collector, and frother (MIBC) were added sequentially with stirring and agitation. The collector concentration was fixed at 5×10^{-5} mol/L in all flotation tests. Flotation was then

carried out for 3 min with aeration. The froth product and tailings were filtered, dried, weighed, and the recovery was calculated. Each test was repeated three times, and the average value was reported.

3. Result and discussion

3.1. Optimized molecular structures of collectors

After geometric optimization, the molecular structures of the four collectors are shown in Fig. 2 In the SBX anion, the bond lengths of C—S and C=S are similar (1.704 Å and 1.698 Å, respectively). Due to the formation of a conjugated S—C—S macro-π bond, the properties of the two sulfur atoms become similar; the C—S bond is slightly longer and weaker, making its S1 atom more susceptible to interact with metal ions on the mineral surface. For ADD, the P—S and P=S bonds can also form a conjugated macro-π bond, and the sulfur atom in the single bond exhibits higher activity due to its longer bond length. In the DDTC anion, a conjugated macro-π bond also exists between the C—S and C=S bonds. Z-200 does not easily ionize in water and does not readily undergo electrostatic adsorption; its structure contains one less active sulfur atom compared to the other collectors, and its C=S bond is the longest, corresponding to the highest activity of its sulfur atom.

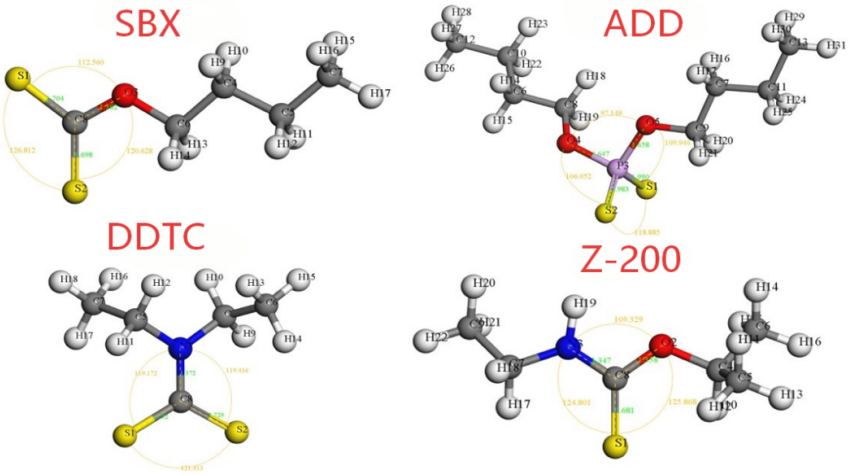

Fig. 2. Optimized structures of collectors

The longitudinal comparison of the characteristic bond lengths of the functional groups of the four collectors is shown in Table 2. Compared with the other three collectors, the central atom of the functional group of ADD is phosphorus. The bond lengths of its P-S and P=S bonds are significantly longer than the corresponding C-S and C=S bonds of the other collectors, indicating that in the $-O_2PS_2$-type functional group represented by ADD, the chemical bonds of the active atoms are the weakest and exhibit the highest reactivity. For the $-NCS_2^-$ type collector represented by DDTC, its bond lengths are second only to those of the $-O_2PS_2^-$ type and are longer than those of the $-OCS_2^-$ type (SBX), indicating that replacing oxygen with nitrogen in the functional group structure can moderately increase bond lengths, thereby enhancing the chemical activity of the coordinating atoms. For the ester collector represented by Z-200, its bond lengths are the shortest and the bond strengths are the strongest, resulting in the weakest interaction ability with metal atoms on the mineral surface.

3.2. Frontier orbital symmetry matching between collector molecules and mineral surfaces

Bond length analysis can preliminarily reflect the properties of reagents, but it is difficult to accurately explain their adaptability to different mineral surfaces. Yu et al (2024) systematically investigated the interactions between flotation reagents and mineral surfaces based on coordination chemistry, providing a theoretical foundation for understanding the adsorption coordination mechanism. By analyzing the frontier rbitals of reagents and mineral surfaces, the matching relationship between them can be further revealed at the electronic level. According to frontier orbital theory (Fukui, 1982), the reactivity and selectivity of molecules primarily depend on the characteristics of their frontier orbitals.

Table 2. Bond lengths of functional groups of optimized collector ions

Functional group type	Name	Bond length (Å)			
		R(P/C-S1)	R(P/C=S2)	R(P/C-O1/N1)	R(P/C-O2)
—OCS_2^-	Sodium n-Butyl Xanthate (SBX)	1.704	1.698	1.382	\
—$O2PS_2^-$	Ammonium Dibutyl Dithiophosphate (ADD)	1.990	1.983	1.647	1.658
—NCS_2^-	Sodium Diethyl Dithiocarbamate (DDTC)	1.732	1.729	1.372	\
NOCS	O-Isobutyl N-Ethyl Thionocarbamate (Z-200)	\	1.682	1.344	1.357

Such DFT-based analysis has been successfully applied to investigate the structure-reactivity relationship of thiophosphorus acids as flotation collectors with sulfide minerals (Liu et al., 2013), with its core concept being the symmetry matching of molecular orbitals. In this study, HOMO and LUMO orbital calculations were performed on four types of collector molecules (SBX, ADD, DDTC, and Z-200), as well as on the surface structures of acanthite, pyrite, and sphalerite.

As shown in Fig. 3, the HOMO shapes of the ionic states of the four collectors are similar, with the electron cloud mainly concentrated on the sulfur atoms. SBX, ADD, and DDTC each contain two coordinating sulfur atoms, while Z-200 contains only one; oxygen atoms also contribute to the HOMO orbitals of the first three reagents. The HOMO of SBX, ADD, and DDTC is mainly composed of pz orbitals of sulfur atoms, whereas the HOMO of Z-200 primarily originates from the py orbital of sulfur. Both types are π-type delocalized orbitals.

The LUMO orbitals of SBX, DDTC, and Z-200 exhibit a side-by-side distribution, mainly contributed by atoms such as S/O/C, S/N/C, and S/O/C/N, respectively, with the atoms in Z-200 arranged in a nearly planar triangle. The LUMO of ADD is a head-to-head S–P σ-bond. The LUMO of SBX and DDTC are py orbitals, Z-200 has a pz orbital (both π-type), and ADD has a px orbital (σ-type).

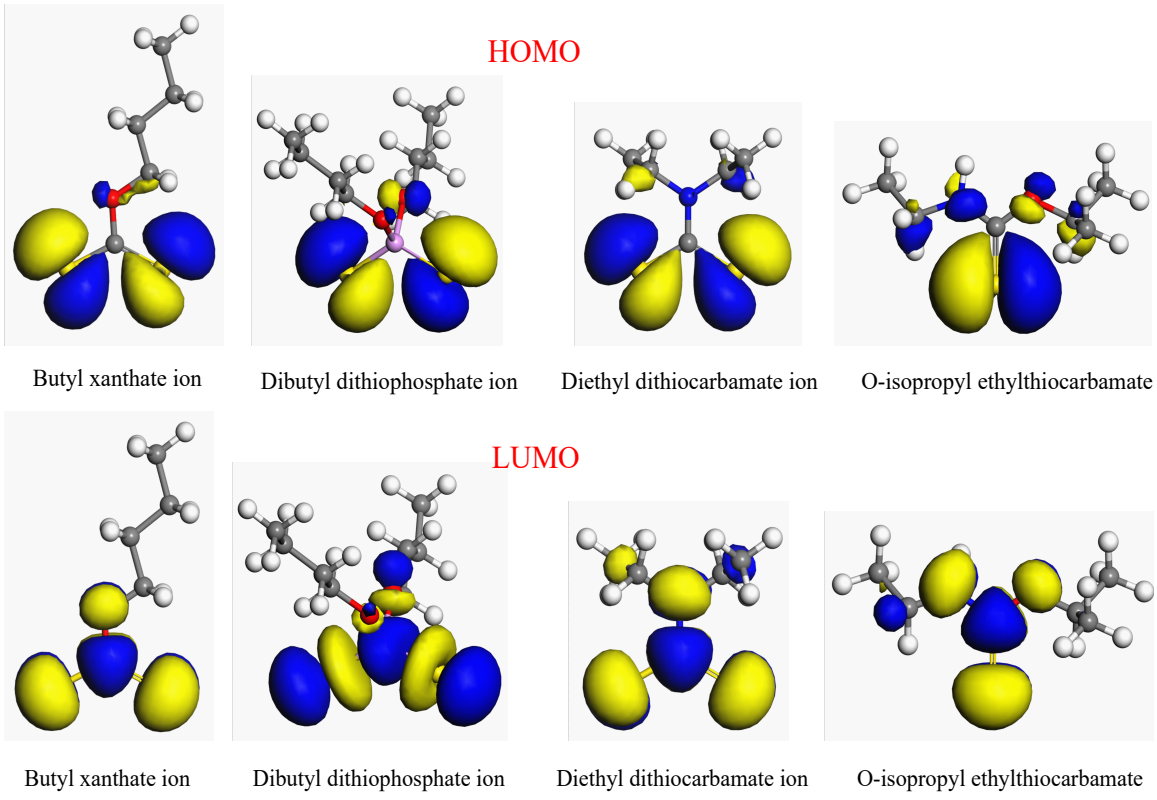

Fig. 3. HOMO and LUMO orbital configurations of the four collectors

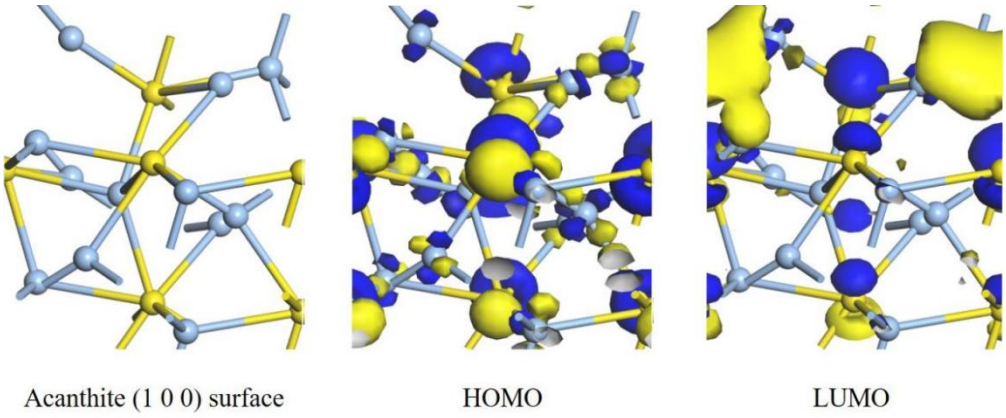

Fig. 4. Frontier orbital configuration of acanthite

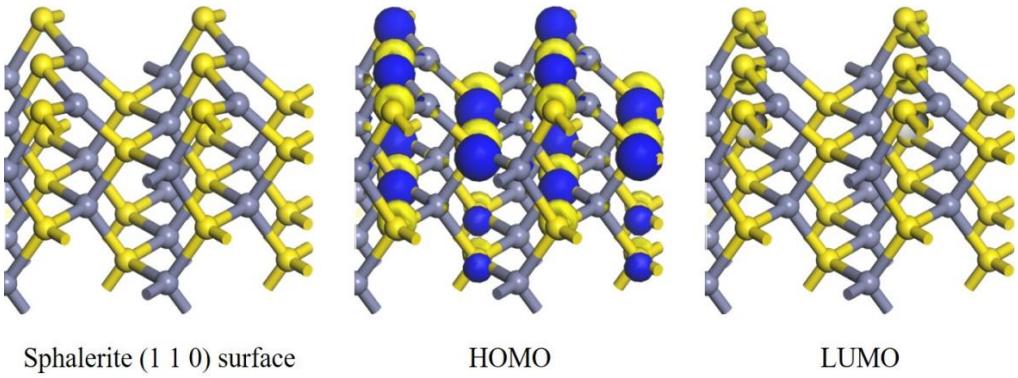

Fig. 5. Frontier orbital configuration of sphalerite

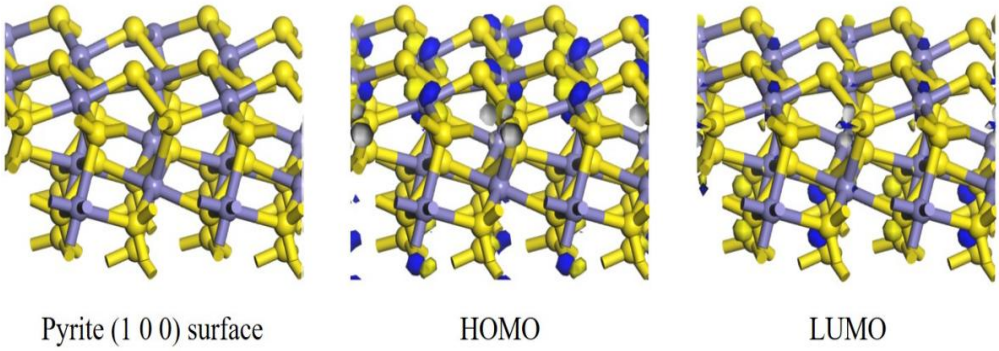

Fig. 6. Frontier orbital configuration of pyrite

Figs. 4-6 show the optimized frontier orbital configurations of acanthite, sphalerite, and pyrite, respectively. On the acanthite surface, there are two types of Ag atoms: three-coordinated (sp^2-like) and four-coordinated (sp^3-like), possibly corresponding to Ag^+ and Ag^{2+}. Its HOMO is contributed by the dxy (π-type) of three-coordinated Ag and the dyz (σ-type) of four-coordinated Ag; the LUMO is formed by hybridization of the dxz of three-coordinated Ag with the 3p orbital of S. For three-coordinated Ag, its dxy (HOMO) matches the py (LUMO) of SBX and DDTC, and its dxz (LUMO) coordinates with the pz (HOMO) of SBX, ADD, DDTC and the py of Z-200. For four-coordinated Ag, the px (LUMO) of ADD can coordinate with its dyz (HOMO), forming a σ-bond, while the pz (HOMO) of ADD donates electrons to the LUMO of four-coordinated Ag, forming a back-donation π-bond. The HOMO of sphalerite is mainly composed of S 3p, with a small contribution from Zn dxy (π-type), and can form weak back-donation π bonds with the py LUMO of SBX and DDTC; its LUMO consists of diffuse Zn 4s and S 3s orbitals, which are spatially extended rather than localized on surface atoms, making them

inherently difficult to visualize in frontier orbital plots. This is consistent with previous DFT studies on sphalerite surfaces (Feng et al., 2024; Mohseni et al., 2018), which also reported that these diffuse orbitals do not actively participate in bonding with collectors. The pz/py HOMO orbitals of the four collectors are therefore difficult to match with the LUMO of sphalerite. The HOMO of pyrite is primarily composed of Fe dxz and S 3p, showing good symmetry matching with the pz LUMO of Z-200; its LUMO mainly originates from Fe dyz (σ-type) and can coordinate with the pz HOMO of SBX, ADD, DDTC and the py HOMO of Z-200. The matching results are summarized in Table 3.

Table 3. Frontier orbital matching between collectors and minerals

Collector	Mineral type and orbital (√: orbital matching; ×: orbital mismatching)							
	Acanthite(three-coordinated)		Acanthite(four-coordinated)		Sphalerite		Pyrite	
	HOMO	LUMO	HOMO	LUMO	HOMO	LUMO	HOMO	LUMO
SBX	√	√	×	×	√	×	√	×
ADD	×	√	√	×	×	×	×	×
DDTC	√	√	×	×	√	×	√	×
Z-200	√	√	×	×	×	×	√	√

According to the analysis in Table 3, both SBX and DDTC can coordinate with the HOMO orbitals of the three mineral surfaces and form back-donation π bonds, resulting in low adsorption selectivity and poor separation efficiency. Z-200 exhibits good orbital matching with pyrite and also shows some matching with the frontier orbitals of acanthite, but its selectivity for acanthite remains insufficient. In contrast, ADD can simultaneously form σ bonds with the LUMO orbitals of three-coordinated Ag on acanthite and form back-donation π bonds with the HOMO orbitals of four-coordinated Ag, providing more adsorption sites and better selectivity on the acanthite surface. This dual-site anchoring configuration provides a more stable adsorption geometry compared to single-site adsorption, as the two bonds collectively restrict the rotational freedom of the collector molecule on the mineral surface. The σ-bond anchors ADD to the three-coordinated Ag site, while the π-bond simultaneously stabilizes the adsorption through interaction with the four-coordinated Ag site. However, orbital matching only indicates the theoretical possibility of coordination between the two; practical flotation also requires comprehensive consideration of factors such as interaction energy and steric hindrance.

3.3. Comparison of frontier orbital energies between collector molecules and mineral surfaces

According to frontier orbital theory, the strength of intermolecular interactions is directly related to the proximity of the energy levels of their frontier orbitals. Specifically, the closer the energy of a molecule's HOMO is to that of another molecule's LUMO, the easier it is for electron transfer and bonding to occur between them (Using fractional charges for computing fukui functions in molecular and periodic systems, n.d.). Therefore, the collecting ability can be evaluated by calculating the differences in HOMO and LUMO orbital energies between the collector and the mineral, i.e., the frontier orbital energy difference ΔE; a smaller ΔE generally indicates a stronger interaction. Here, ΔE_1 is defined as the absolute difference between the collector's HOMO energy and the mineral's LUMO energy, and ΔE_2 is defined as the absolute difference between the collector's LUMO energy and the mineral's HOMO energy. The results are summarized in Table 4-5.

It can be seen from Table 4-5 that the ΔE_2 values of all systems are generally higher than their ΔE_1 values, indicating that the interaction between the LUMO orbitals of the collectors and the HOMO orbitals of the minerals is relatively weak overall, which is consistent with literature reports (Pearson, 1972). Comparing different collectors, ADD exhibits the smallest ΔE_1 with acanthite, showing a strong electron-donating ability. However, its ΔE_1 with pyrite is even smaller (0.0148 eV), indicating that it also has a good bonding affinity for pyrite. Nevertheless, judging collecting performance solely based on ΔE_1 is not comprehensive; the reverse electron effect reflected by ΔE_2 also plays an important role in adsorption selectivity. The ΔE_2 values of ADD with sphalerite and pyrite are much larger than those of the other three collectors, indicating that its LUMO orbital does not readily accept electrons from the

HOMO orbitals of these two minerals. A large ΔE_2 indicates that electron transfer from the mineral HOMO to the collector LUMO is energetically unfavorable. For ADD, the ΔE_2 values with sphalerite (6.1285 eV) and pyrite (5.9855 eV) are substantially larger than those of the other collectors, suggesting that back-donation π-bond formation is effectively blocked on these two mineral surfaces, which contributes to the high selectivity of ADD. In contrast, its ΔE_2 with acanthite is relatively small, suggesting good energy level matching between them, which is consistent with the orbital symmetry analysis in the previous section. The magnitude of ΔE_2 is also related to the strength of the back-donation π bond, thereby affecting mineral selectivity. Thus, ADD achieves both good collecting ability and favorable selectivity for acanthite.

Table 4. Frontier orbital energies of collectors

Collectors	Frontier orbital energy(eV)		$\Delta E_1=\lvert E_{HOMO\text{-}collector}r\text{-}E_{LUMO\text{-}mineral}\rvert$			$\Delta E_2=\lvert E_{HOMO\text{-}mineral}\text{-}E_{LUMO\text{-}collector}\rvert$		
	HOMO	LUMO	Acanthite	Sphalerite	Pyrite	Acanthite	Sphalerite	Pyrite
SBX	−4.2562	−1.1158	0.5426	1.1295	0.5868	4.3795	4.4996	4.3566
ADD	−4.6514	0.5131	0.1438	1.5247	0.1916	5.6084	6.1285	5.9855
DDTC	−3.8635	−1.0054	0.9317	0.7368	0.9795	4.4899	4.7201	4.5771
Z-200	−5.3441	−1.2898	0.5489	2.2174	0.5011	4.5054	4.3256	4.1826

Table 5. Frontier orbital energies of minerals

Mineral sample	Frontier orbital energy(eV)	
	HOMO	LUMO
Acanthite	−5.0953	−4.7952
Sphalerite	−5.6154	−3.1267
Pyrite	−5.4724	−4.8430

3.4. Interaction model of collectors with silver, zinc, and iron ions

We acknowledge that the simplified metal ion model is intended to capture the intrinsic affinity difference between the collectors and different metal ions, rather than to provide absolute adsorption energies for real mineral surfaces. The relative order of adsorption energies is consistent with the flotation results, suggesting that the model is adequate for comparative screening purposes. The present results should therefore be interpreted as a qualitative guide rather than quantitative predictions.

In the flotation system, collector anions typically coordinate with metal ions exposed on the mineral surface (Zhang et al., 2023). In addition to metal ions, sulfide ions on the sulfide mineral surface also contribute significantly to the frontier orbitals (Fig. 7(c)). Therefore, sulfide ions also have a certain influence during the coordination process. This study establishes an adsorption model containing only metal ions and collectors, ignoring the interference of surrounding sulfide ions on the adsorption process, thereby comparing the interaction strengths of different collectors with metal ions. Fig. 7 shows the interaction configurations of collectors with Ag^+, Zn^{2+}, and Fe^{2+}, respectively.

Table 6 shows that the interaction distances between the four collectors and Fe^{2+} are the shortest, indicating the strongest affinity for Fe^{2+}; while the distances for Ag^+ are relatively longer, indicating difficulty in binding with silver ions, which partially explains the generally low recovery of silver minerals in practice. The adsorption energy analysis shows that DDTC has extremely high adsorption energies for Fe^{2+} and Zn^{2+}(-925.53 and -729.53 kJ/mol, respectively), which easily leads to separation difficulties, and the addition of lime to depress pyrite in actual flotation further reduces the floatability of silver minerals. Z-200 exhibits low adsorption energies for all three ions, with an adsorption energy of only -119.9588 kJ/mol for Ag^+, making it susceptible to competitive adsorption in the pulp, which is unfavorable for silver mineral flotation. SBX and ADD have similar adsorption energies, but ADD has a slightly lower (more negative) adsorption energy for Ag^+ by about 5 kJ/mol, and its adsorption for Zn^{2+} and Fe^{2+} is weaker than that of SBX, indicating better selectivity for silver ions.

3.5. Effect of collectors on the flotation behavior of acanthite

3.5.1. Effect of different collectors on the flotation behavior of acanthite

Previous studies have extensively investigated collectors for acanthite flotation. Traditionally, xanthate has been the most commonly used collector for acanthite; however, due to its insufficient selectivity, the recovery of associated silver in complex polymetallic sulfide ores is often unsatisfactory. Research indicates that acanthite exhibits good floatability in weakly alkaline media (pH 9-10), and the saturated adsorption capacity of ADD on the acanthite surface is superior to that of ethyl xanthate and DDTC, demonstrating that the dithiophosphate structure has a stronger affinity for silver minerals (Chen, 2022); According to the experimental results shown in Fig. 8, DDTC exhibits the poorest flotation performance for acanthite, with a maximum recovery of only 67.77%. The flotation performances of SBX and Z-200 for acanthite are similar, but both are slightly lower than that of ADD, which is consistent with the frontier orbital theory conclusion that ADD has the best separation effect for silver.

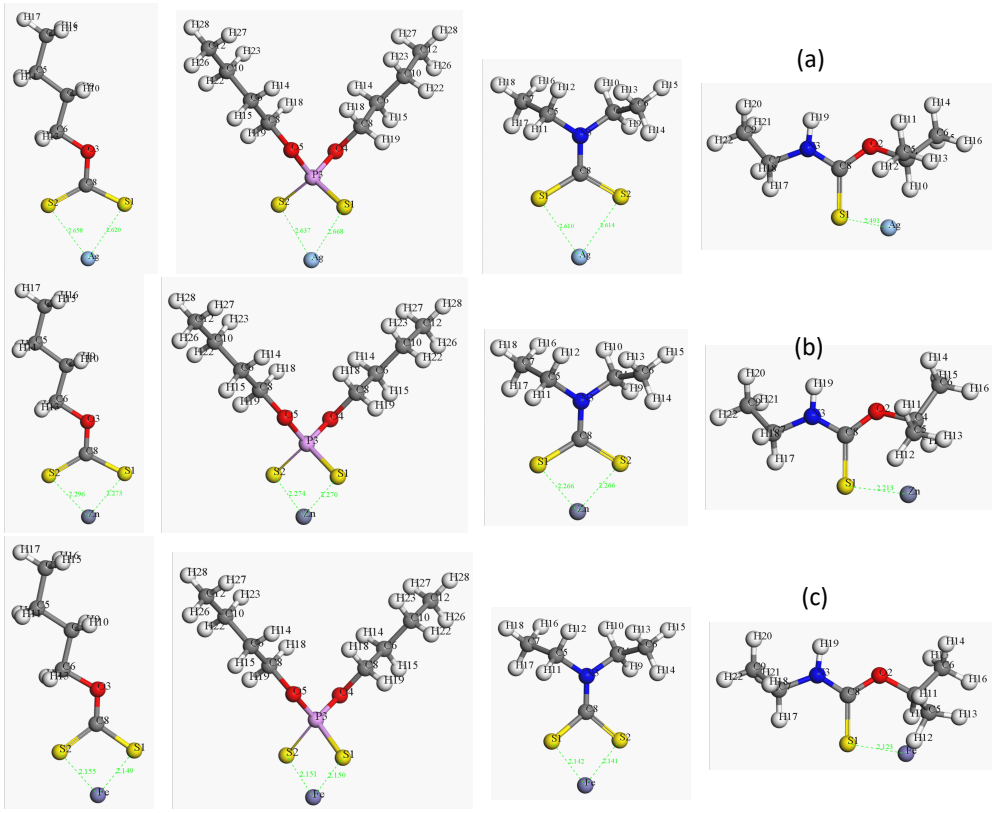

Fig. 7. Interaction configurations of collectors with metal ions (a) collectors with Ag^{+} (b) collectors with Zn^{2+} (c) collectors with Fe^{2+}

3.5.2. Effect of ADD on the flotation behavior of different minerals

Dialkyl dithiophosphates (DTP) are a class of sulfide mineral collectors widely used in industrial flotation. Among them, O,O-dialkyl dithiophosphates (such as ADD in this study) contain both electron-donating groups and coordinating sulfur atoms in their molecular structure, enabling them to

Table 6. Bond lengths and adsorption energies of collectors with metal ions

Name	Bond length (Å)						Adsorption energy (kJ/mol)		
	Ag-S1	Ag-S2	Zn-S1	Zn-S2	Fe-S1	Fe-S2	Ag^{+}	Zn^{2+}	Fe^{2+}
SBX	2.620	2.658	2.273	2.296	2.149	2.155	−214.1683	−674.5047	−872.6829
ADD	2.668	2.637	2.270	2.274	2.150	2.151	−219.7874	−658.9242	−844.4351
DDTC	2.610	2.614	2.266	2.266	2.142	2.141	−228.2459	−729.5333	−925.5334
Z-200	2.491	/	2.213	/	2.123	/	−119.9588	−450.8393	−629.3223

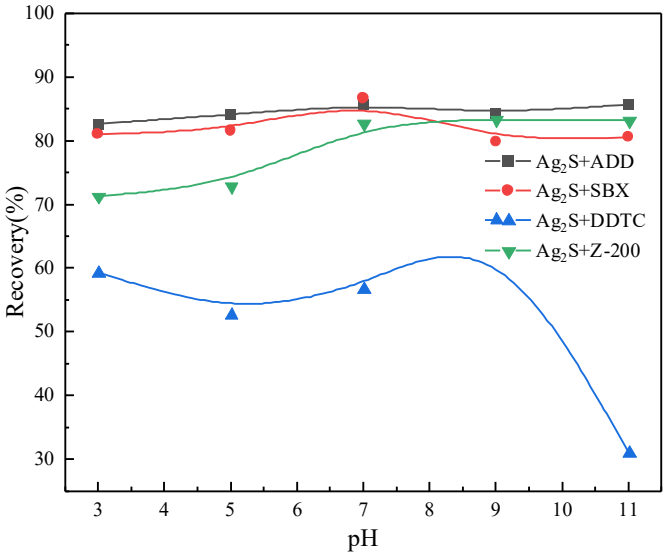

Fig. 8. Effect of different collectors on the floatability of acanthite

form stable covalent bonds with metal ions on sulfide mineral surfaces. They have thus attracted considerable attention in the study of precious metal sulfide flotation. Based on frontier orbital theory analysis, ADD, with its unique bidentate coordination structure, forms a favorable σ-π synergisticadsorption mode with silver atoms in different coordination states on the acanthite surface, theoretically predicting that ADD possesses high collecting ability and selectivity for acanthite. However, in actual flotation systems, mineral behavior is not only controlled by the electronic structure of reagent molecules but also influenced by the coupled effects of various factors such as pulp pH, type of modifier (e.g., CaO) and its hydrolysis species, and mineral surface dissolution characteristics (du Plessis et al., 2019). In this section, single-mineral flotation tests were conducted to investigate the effect of ADD on the flotation recovery of acanthite, sphalerite, and pyrite under different pH conditions. The aim was to verify the selectivity predicted by frontier orbital theory and to provide experimental evidence for the efficient separation of associated silver minerals in complex polymetallic sulfide ores. According to the experimental results shown in Fig. 9, ADD exhibits relatively strong collecting ability for pyrite under acidic conditions, but its recovery decreases significantly with increasing pH. Sphalerite shows low recovery under acidic conditions, and its floatability under alkaline conditions is similar to that of pyrite. In contrast, acanthite exhibits good floatability over a wide pH range, which is consistent with the description in the previous section.

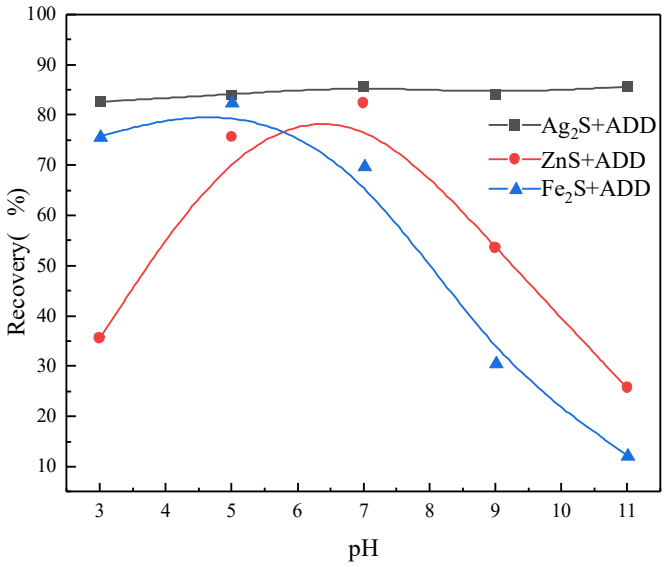

Fig. 9. Effect of ADD on the floatability of different minerals under various pH conditions

3.5.3. Effect of ADD on the flotation behavior of mixed minerals

To verify the actual separation performance of ADD in complex mineral systems, flotation tests were conducted on a mixed mineral sample consisting of acanthite, sphalerite, and pyrite in a mass ratio of 1:1:1, with a total mass of 3.0 g. The tests were carried out at pH 8, a collector concentration of 5×10^{-5} mol/L, and an MIBC dosage of 10 mg/L, and were compared with the industrially common collector SBX. The results are shown in Table 7. When SBX was used as the collector, the concentrate yield was relatively high, but the silver grade was only 16.08% and the silver recovery was 73.30%. Meanwhile, a large amount of sphalerite and pyrite reported to the concentrate, exhibiting indiscriminate strong collecting ability. In contrast, when ADD was used as the collector, the concentrate yield decreased to 64.14%, the silver grade increased to 19.56%, and the silver recovery increased to 85.91%. Moreover, the flotation of sphalerite was significantly suppressed, indicating that ADD achieves superior selective separation performance while ensuring a high silver recovery.

Table 7. Flotation separation results of ADD and SBX on ternary mixed mineral system

Collectors	Product	Yield (%)	Grade (%)			Recovery (%)		
			Zn	Ag	Fe	Zn	Ag	Fe
ADD	Concentrate	64.14	11.16	19.56	17.89	31.79	85.91	73.52
	Tailings	35.86	42.81	5.74	11.53	68.21	14.09	26.48
SBX	Concentrate	70.22	20.72	16.08	15.51	69.14	73.30	71.16
	Tailings	29.78	22.85	12.83	14.82	30.86	26.70	28.84

4. Conclusions

(1) Frontier orbital matching analysis indicates that ADD can form a σ-bond with the LUMO of three-coordinated Ag via its px LUMO, and a back-donation π-bond with the HOMO of four-coordinated Ag via its pz HOMO on the acanthite surface, providing the most adsorption sites and the best coordination effect. Although SBX and DDTC can match with multiple minerals, they exhibit poor selectivity. Z-200 matches with pyrite and acanthite but mainly forms σ-bonds, resulting in relatively weak interaction.

(2) The frontier orbital energy difference calculation shows that ADD has the smallest ΔE_1 (0.1438 eV) between its HOMO and the LUMO of acanthite, indicating the strongest electron-donating ability. Its ΔE_2 values with sphalerite and pyrite (6.1285 eV and 5.9855 eV, respectively) are much larger than those of the other collectors, indicating that back-donation π-bonds play a key role in its selectivity. This theoretically explains ADD's high collecting ability for acanthite and its low affinity for sphalerite and pyrite.

(3) The adsorption energies of the collectors with metal ions follow the order: Z-200 (–119.96 kJ/mol) < SBX (–214.17 kJ/mol) < ADD (–219.79 kJ/mol) < DDTC (–228.25 kJ/mol). Considering their adsorption selectivity for Zn^{2+} and Fe^{2+}, ADD maintains relatively strong adsorption for Ag^{+} while exhibiting the weakest adsorption for impurity ions, making it the most suitable collector for acanthite among the four. The selectivity index (Ag recovery vs. Zn recovery) is 2.70 for ADD, compared to 1.06 for SBX.

(4) Single-mineral and mixed-mineral flotation tests confirmed that ADD achieves the highest acanthite recovery and superior separation performance over SBX, with significantly improved silver grade and recovery while effectively depressing sphalerite.

Acknowledgements

The authors gratefully acknowledge the support from the National key research and development plan (No. 2022YFC2904504). The Science and technology research project of Jiangxi Provincial Department of Education (No. GJJ2200864).

References

ACARKAN N., BULUT G., GUL A., KANGAL O., KARAKAS F., KOKKILIC O., ONAL G., 2011. *The effect of collector's type on gold and silver flotation in a complex ore*. Sep. Sci. Technol. 46(2), 283–289.

CHEGINI M., ALLAHKARAMI E., ALLAHKARAMI E., 2024. *Unlocking high-value metals: Efficient flotation techniques for lead and silver ore*. Results Eng. 24, 103083.

CHEN D. X., JUN J., 2017. *Mineralogical characterization of a polymetallic sulfide ore to improve silver recovery*. J. Wuhan Univ. Technol. (Mater. Sci.) 32(3), 501–507.

CHEN J., LI Y., 2022. *Orbital symmetry matching study on the interactions of flotation reagents with mineral surfaces*. Miner. Eng. 179.

CHEN Y., 2022. *Comprehensive recovery of associated gold, silver and copper from an iron ore in Qinghai*. Multipurpose Util. Miner. Resour. 0(4), 12.

CUI W., CHEN J., LI Y., CHEN Y., ZHAO C., 2020. *Interactions of xanthate molecule with different mineral surfaces: a comparative study of Fe, Pb and Zn sulfide and oxide minerals with coordination chemistry*. Miner. Eng. 159.

DING K., ZHAO G., QIU T., QIU X., YAN H., WU H., YANG W., YAN S., LIN L., 2025. *Adsorption of dithiophosphate-type collectors with different substituent types on the acanthite surface in the CaO system*. Rare Met. 44(12), 10981–10997.

DING M., LIU Y., CHEN J., LI Y., 2024. *DFT study on the effects of substituents on the structure and properties of dithiophosphate collectors*. Int. J. Quantum Chem. 124(4).

DRIF B., TAHA Y., HAKKOU R., BENZAAZOUA M., 2018. *Recovery of residual silver-bearing minerals from low-grade tailings by froth flotation: the case of zgounder mine, morocco*. Miner. 8(7), 273.

FENG Y., CHEN Y., CHEN J., 2024. *The mechanism of surface activation in sphalerite by metal ions with d10 electronic configurations: experimental and DFT study*. Appl. Surf. Sci. 649, 159181.

FOUCAUD Y., BADAWI M., FILIPPOV L., FILIPPOVA I., LEBEGUE S., 2019. *A review of atomistic simulation methods for surface physical-chemistry phenomena applied to froth flotation*. Miner. Eng. 143.

FUKUI K., 1982. *Role of frontier orbitals in chemical reactions*. Science 218(4574), 747–754.

GONG C., LI H., WANG H., ZHANG C., ZHUANG Q., WANG A., XU Z., CAI W., LI R., LI X., ZANG Z., 2024. *Silver coordination-induced n-doping of PCBM for stable and efficient inverted perovskite solar cells*. Nat. Commun. 15.

GUNER M. K., LODE S., MALAFEEVSKIY N., AASLY K., KOWALCZUK P., 2024. *Mixed thiol collector system in the flotation of copper ore using the REFLUX flotation cell (RFC)*. Miner. Eng. 216, 108843.

HUNG A., YAROVSKY I., RUSSO S. P., 2004. *Density-functional theory of xanthate adsorption on the pyrite FeS2 (100) surface*. Philos. Mag. Lett. 84(3), 175–182.

IGNATKINA V. A., BOCHAROV V. A., PUNTSUKOVA B. T., ALEKSEYCHUK D. A., 2010. *Analysis of selectivity of thionocarbamate combinations with butyl xanthate and dithiophosphate*. J. Min. Sci. 46(3), 324–332.

IGNATKINA V. A., BOCHAROV V. A., D'YACHKOV F. G., 2015. *Enhancing the disparity in flotation properties of nonferrous metal sulfides using sulfhydryl collecting agents with different molecular structures*. J. Min. Sci. 51(2), 389–397.

LI J., JI C. C., XIE X., KANG B. W., FAN P. Q., 2020. *Experimental study on flotation separation of zinc and silver from a silver-rich zinc concentrate in Yunnan*. Chin. J. Process Eng. 20(8), 938–946.

LI Y., LIU Y., CHEN J., ZHAO C., 2020. *Structure-activity of chelating collectors for flotation: a DFT study*. Miner. Eng. 146.

Lime use and functionality in sulphide mineral flotation: a review, 2019. Miner. Eng. 143, 105922.

LIU G., XIAO J., ZHOU D., ZHONG H., CHOI P., XU Z., 2013. *A DFT study on the structure-reactivity relationship of thiophosphorus acids as flotation collectors with sulfide minerals: implication of surface adsorption*. Colloids Surf. A 434, 243–252.

MAKANZA A. T., VERMAAK M. K. G., DAVIDTZ J. C., 2008. *The flotation of auriferous pyrite with a mixture of collectors*. Int. J. Miner. Process. 86(1–4), 85–93.

MOHSENI M., ABDOLLAHY M., POURSALEHI R., KHALESI M., 2018. *An insight into effect of surface functional groups on reactivity of Sphalerite (110) surface with Xanthate collector: a DFT study*. J. Min. Environ. 9, 431–439.

NEISIANI A. A., CHELGANI S. C., 2024. *Biodegradable acids for pyrite depression and green flotation separation – an overview*. Crit. Rev. Biotechnol. 44(6), 1226–1240.

PEARSON R. G., 1972. *Orbital symmetry rules for unimolecular reactions*. J. Am. Chem. Soc. 94(24), 8287–8293.

PIENAAR D., JORDAAN T., MCFADZEAN B., O'CONNOR C. T., 2019. *The synergistic interaction between dithiophosphate collectors and frothers at the air-water and sulphide mineral interface*. Miner. Eng. 138, 125–132.

SHI D., LI W., HAN Y., 2023. *Fluorite flotation separation from bastnaesite via an eco-friendly polymer as a depressant and insight into its mechanism of adsorption*. J. Mol. Liq. 376, 121368.

SVERDRUP H., KOCA D., RAGNARSDOTTIR K. V., 2014. *Investigating the sustainability of the global silver supply, reserves, stocks in society and market price using different approaches*. Resour. Conserv. Recycl. 83, 121–140.

TERCERO N., NAGARAJ D. R., FARINATO R., 2019. *A critical overview of dithiophosphinate and dithiophosphate interactions with base metal sulfides and precious metals*. Min. Metall. Explor. 36(1), 99–110.

TIU G., GHORBANI Y., JANSSON N., WANHAINEN C., BOLIN N.-J., 2023. *Quantifying the variability of a complex ore using geometallurgical domains*. Miner. Eng. 203.

TKACHEV A. V., RUNDQVIST D. V., VISHNEVSKAYA N. A., 2017. *Metallogenic specialization of supercontinent cycles: a case study of silver deposits*. Dokl. Earth Sci. 475(1), 766–770.

VRLÍKOVÁ V., ČABLÍK V., JANÁKOVÁ I., 2020. *Utilization of flotation in copper extraction from polymetallic ore*. GeoSci. Eng. 66(1), 53–59.

WANG K., DI A., ZHANG S., NI L., WANG H., LIU H., HUANG Y., MAO Y., XIE J., ZOU G., HOU H., DENG W., JI X., 2024. *Zinc anode based alkaline energy storage system: recent progress and future perspectives of zinc-silver battery*. Energy Storage Mater. 69, 103385.

WANG L., LI Z., ZHANG H., LYU W., ZHU Y., MA Y., LI F., 2024. *The role of gellan gum in the selective flotation separation of fluorite from calcite: an experimental and molecular dynamics simulation study*. Powder Technol. 432.

YANG W., WANG G., WANG Q., DONG P., CAO H., ZHANG K., 2019. *Comprehensive recovery technology for Te, Au, and Ag from a telluride-type refractory gold mine*. Minerals 9(10), 597.

YU X., YIN Z., CHEN Y., SHEN P., WANG H., MAO Y., LIU D., 2024. *Experimental and DFT study of modified malachite with 2,5-dimercapto-1,3,4-thiadiazole and its response to sulfidization-xanthate behavior*. Colloids Surf. A 693.

ZHANG H., ZHANG F., SUN W., CHEN D., CHEN J., WANG R., HAN M., ZHANG C., 2023. *The effects of hydroxyl on selective separation of chalcopyrite from pyrite: a mechanism study*. Appl. Surf. Sci. 608.

ZHANG H., YU H., SUN W., LIN S., ZHANG C., 2024. *Beneficiation of silver and silver-bearing lead-zinc ores: a review*. Miner. Eng. 208, 108608.

ZHANG W., CAO J., WU S., SUN W., FENG Z., GAO Z., 2022. *Synthesis of selective heteroatomic collectors for the improved separation of sulfide minerals*. Sep. Purif. Technol. 287.

ZHANG X., XU X., ZHANG Y., LIU X., YU J., CHEN X., YANG J., ZUO Q., SHEN P., LIU D., 2024. *Uncovering mechanism of excessive copper ion-activated depressed-sphalerite under moderate alkaline conditions: a combined experimental and DFT investigation*. J. Mol. Liq. 414, N.PAG–N.PAG.

ZHANG Y., CHEN J., 2021. *Sulfidizing behavior of complex lead-silver ore: a flotation study*. Minerals 11(4), 434–445.